Adenosine diphosphate–induced aggregation of human platelets in flow through tubes

II. Effect of shear rate, donor sex, and ADP concentration

David N. Bell, Samira Spain, and Harry L. Goldsmith
McGill University Medical Clinic, Montreal General Hospital Research Institute, Montreal, Quebec H3G 1A4 Canada

ABSTRACT The effect of shear rate on the adenosine diphosphate–induced aggregation of human platelets in Poiseuille flow was studied using the method described in part I (Bell, D. N., S. Spain, and H. L. Goldsmith. 1989. *Biophys. J.* 56:817–828). The rate and extent of aggregation in citrated platelet-rich plasma were measured over a range of mean transit time from 0.2 to 8.6 s and mean tube shear rate, $\bar{G}$, from 41.9 to 1,920 s^{-1}. At 0.2 μM ADP, changes in the single platelet concentration with time suggest that more than one type of platelet–platelet bond mediates platelet aggregation at physiological shear rates. At low $\bar{G}$, a high initial rate of aggregation reflects the formation of a weak bond of high affinity, the strength of which diminishes with time. Here, the fraction of collisions yielding stable doublets, the collision efficiency, reached a maximum of 26%. The collision efficiency decreased with increasing $\bar{G}$ and was accompanied by a progressive delay in the onset of aggregation. However, the gradual expression of a more shear rate–resistant bond at high shear rates and long mean transit times produced a subsequent increase in collision efficiency and a corresponding increase in the rate of aggregation. Although the collision efficiencies here were <1%, the high collision frequencies were able to sustain a high rate of aggregation. At 0.2 μM ADP, aggregate size generally decreased with increasing $\bar{G}$. At 1.0 μM ADP, aggregate size was still limited at high shear rates even though the rate of single platelet aggregation was much higher than at 0.2 μM ADP. Platelet aggregation was greater for female than for male donors, an effect related to differences in the hematocrit of donors before preparing platelet-rich plasma.

INTRODUCTION

Shear rate is the most important physical parameter governing platelet aggregation in flowing suspensions. It determines the platelet collision frequency, the shear and normal stresses which activate single cells and break up aggregates, and the interaction time of cell–cell and cell–surface collisions. The predilection of white platelet thrombi to form in regions of high wall shear rate in the arterial circulation emphasizes the need to focus on the effect of shear rate on platelet aggregation in well-defined flow. Time-averaged systemic arterial wall shear rate in humans is estimated to range from 50 to 2,000 s^{-1} (Goldsmith and Turitto, 1986), based on a parabolic velocity profile for whole blood. It has been shown in vitro that shear rates <2,000 s^{-1} are not sufficient to activate platelets directly and induce aggregation (Bell and Goldsmith, 1984; Belval and Hellums, 1986; Belval et al., 1984; Chang and Robertson, 1976; Gear, 1982; Yung and Frojmovic, 1982). However, the higher shear rates commonly found in extracorporeal flow devices and vascular prostheses can induce platelet aggregation, release, and lysis, depending on the magnitude of the fluid shear stress and the time of exposure to the shear field (Belval et al., 1984; Brown et al., 1975; Colantuoni et al., 1977; Dewitz et al., 1978; Jen and McIntire, 1984).

The importance of the release of platelet-derived platelet agonists, particularly ADP, in sustaining and enhancing shear-induced platelet aggregation has led to a number of studies on the effect of flow on agonist-induced platelet aggregation. Because high shear stresses activate platelets and induce release, the aggregation of platelets in response to exogenous agonists is generally confined to shear rates and agonist concentrations that are below the threshold for release. Despite variability in the ADP concentration and suspension temperature used, the results of several studies suggest that the aggregation of ADP-stimulated platelets increases with increasing shear rate over the range from 0 to 2,200 s^{-1}. Chang and Robertson (1976) followed the kinetics of both Brownian motion- and shear-induced aggregation at 25°C in a cylindrical Couette using measurements of suspension turbidity. At 10 μM ADP, the rate of aggregation was shown to increase over the range of shear rate from 10 to 75 s^{-1} and level off thereafter, although shear rates >100 s^{-1} were not tested. The rate of aggregation increased with increasing ADP concentration, reaching a maximum at 100 μM ADP; however, the early stages of aggregation were lost due to a 10 s preshear mixing period. As well, aggregate size and the kinetics of aggregate growth could not be extracted from the changes in suspension turbidity that were used to monitor aggregation. Yung and Froj-

0006-3495/89/11/829/15 $2.00

movic (1982) observed that unstable aggregates which formed at 1.5 μM ADP in a parallel plate Couette at shear rates <150 s^{-1} at 37°C were stable at 5 μM ADP; however, the release of endogenous ADP at the higher level of platelet stimulation would have increased the effective ADP concentration. Again, a brief period of high shear used to mix the ADP and platelets prevented observation of the early stages of the aggregation reaction. We have observed the complete aggregation reaction directly using a microscopic double infusion system that allowed the rapid diffusion of ADP throughout the bulk of a platelet suspension undergoing Poiseuille flow (Bell and Goldsmith, 1984; Bell et al., 1984). In contrast to conventional fixed-volume rotational viscometers and aggregometer cuvettes, such a flowthrough system more closely mimics in vivo conditions. Even though mixing is complete, collisions can occur between platelets at different stages of activation due to differences in cell transit time. At 1 μM ADP at room temperature, the rate and final extent of aggregation after a mean transit time of 27 s increased with increasing mean tube shear rate, $\bar{G}$, over the range 2–54 s^{-1}. Higher shear rates could not be studied at equivalent exposure times to ADP due to the microscopic dimensions of the flow system and constraints on the distance for complete diffusion of ADP. Gear (1982) used a narrow bore tube flow system to bring platelets and agonist together in a Y-junction at high velocity. At 10 μM ADP and at 37°C, it was found that ~50% of the platelets had aggregated within 2–4 s of flow through the reaction tube at $\bar{G}$ = 1,300 or 2,200 s^{-1}, with the rate of aggregation higher at the higher shear rate. Again, the release of endogenous ADP at 37°C would considerably augment the degree of aggregation.

In part I (Bell et al., 1989) we introduced a method for rapidly mixing ADP and platelet suspension before flowing it through fixed lengths of polyethylene tubing at controlled rates. Part II uses this method to follow the kinetics of platelet aggregation in the citrated plasma of a large group of donors over a range of mean tube shear rate from 41.9 to 1,920 s^{-1} at 0.2 and 1.0 μM ADP at room temperature.

EXPERIMENTAL PART

1. Platelet-rich plasma and reagents

Citrated platelet-rich plasma (PRP) was prepared from venous blood drawn from equal numbers of healthy, age-matched male and female volunteers, as described in part I. Rapidly mixed suspensions of PRP and ADP at final concentrations of 3×10^5 cells μl^{-1} and 0.2 or 1.0 μM ADP flowed through 1.19 or 0.76 mm i.d. polyethylene tubes (Fig. 1, part I) at preset volume flow rates from 13 to 155 $\mu l\ s^{-1}$, corresponding to mean tube shear rates (Eq. 1, part I) from 41.9 to 1,920 s^{-1}.

Thromboxane B_2 (TXB_2) was measured to a lower limit of 50 pg ml^{-1} in the plasma of selected experiments by radioimmunoassay (RIA) using ^{3}H-TXB_2 (New England Nuclear, Lachine, Quebec). Approximately 800 μl of unfixed effluent platelet suspension were collected into 1-ml plastic syringes and immediately filtered free of cells using 0.2-μm pore syringe filter units (Millex-GS, Millipore, Mississauga, Ontario). The filtered plasma was incubated for 20 min at 37°C and stored at −20°C until the RIA was performed.

2. Analysis of data

The number concentration and volume of single platelets and aggregates were measured using the electronic particle counting and sizing system described in part I to generate 250 class log-volume histograms over the volume range from 1 to 10^5 μm^3. Average log-volume histograms were generated from multiple donors at each mean transit time after the histograms of individual donors were transformed into equivalent histograms using the average of the mean single platelet volume and standard deviation of all donors concerned. The mean normalized volume fraction of the ith class is given by $\bar{\Phi}(x_i) = [\bar{N}(x_i)\, v(x_i)/\bar{N}(x_m)\, v(x_m)]$, where $\bar{N}(x_i)$ is the mean normalized particle concentration per histogram class, and $\bar{N}(x_m)$ and $v(x_m)$ (see Nomenclature in part I) are the respective mean normalized number concentration and volume of the class of maximum concentration, m, at $\bar{t} = 0$ s. Details of the transformation and averaging are given elsewhere (Bell, 1988). The ultimate effect of these procedures is to provide an estimate of the changes in particle volume in relation to the mean single platelet volume and standard deviation, as opposed to simply averaging changes in absolute volume.

Statistics of the linear single platelet volume distribution and tests of log-normality were computed as described in part I.

RESULTS

1. Distribution of single platelet volume

40 male and 40 female donors of age 31 ± 11 (±SD, n = 57) and 30 ± 6 (n = 56) years, respectively, were used in a total of 113 experiments involving nine shear rates. The data are grouped according to sex due to large differences in the degree of aggregation between male and female donors.

Table 1 shows average statistics of the individual single platelet log-volume histograms. The distribution of single platelet volume in citrated PRP was log-normal according to the Kolmogorov-Smirnov one sample test for 74% of 47 male donors and 60% of 42 female donors. As discussed in part I, all volumes are those of the equivalent sphere due to the variation in single platelet and aggregate shape. Platelet volume distributions from both male and female donors that were log-normal shared the same average mean volume, $\bar{\mu}$ = 7.3 μm^3. The average standard deviation, mode, and median of the two sexes were also virtually identical, and neither group exhibited significant skewing or kurtosis. For both groups of donors, the average measures of platelet volume of distributions that were rejected by the K-S test were always greater than those of their log-normal counterparts, although none of

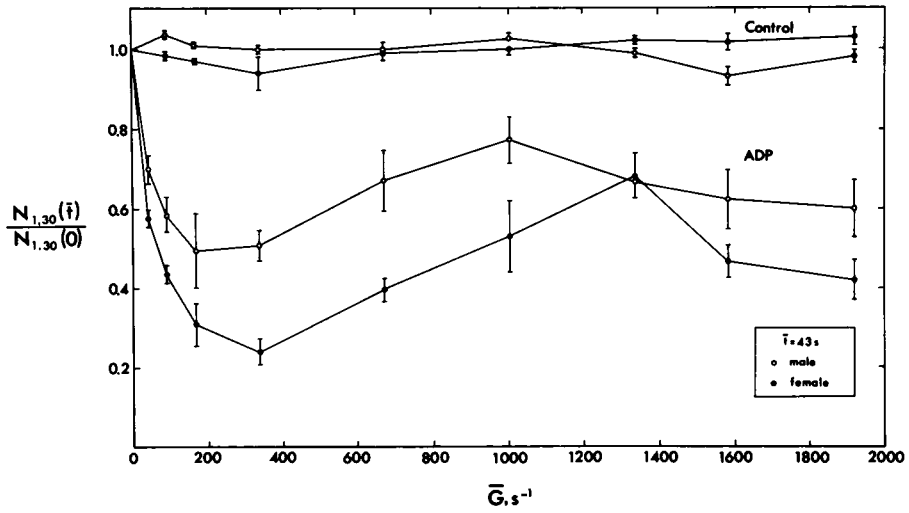

FIGURE 1 Single platelet concentration vs. mean tube shear rate. The normalized single platelet concentration, $N_{1,30}(\bar{t})/N_{1,30}(0)$, (±SEM) after $\bar{t}$ = 43 s exposure to 0.2 μM ADP as a function of mean tube shear rate for male and female donors. In the control runs modified Tyrodes was infused instead of ADP.

the differences was statistically significant. The apparent increase in cell volume of the rejected distributions coincided with significant positive skewing ($g_1 > 0$, $P < 0.02$) and an increased tendency toward leptokurtosis ($g_2 > 0$, $P < 0.01$).

2. Single platelet concentration

a. Effect of shear rate and donor sex

The mean single platelet concentration before shearing was 279,000 ± 23,000 cells μl^{-1} (±SD) for the male donors and 278,000 ± 34,000 cells μl^{-1} for the female donors. Fig. 1 shows the single platelet concentration after $\bar{t}$ = 43 s exposure to 0.2 μM ADP, $N_{1,30}(\bar{t})$, normalized to a control at $\bar{t}$ = 0 s, $N_{1,30}(0)$, as a function of the mean tube shear rate. A two-way analysis of variance verified that the extent of aggregation of platelets from female donors was significantly greater than that of platelets from male donors ($P < 0.001$) over the range of shear rate $41.9 \leq \bar{G} \leq 1{,}920$ s^{-1} (Bell, 1988). The sex difference was greatest at $\bar{G}$ = 335 s^{-1} where 76 ± 3.4% (SEM, n = 6) of single platelets from the female donors but only 49 ± 3.9% (n = 6) of those from male donors had aggregated. Significant changes ($P < 0.001$) in the single platelet concentration as a function of mean tube shear rate produced a similar pattern of aggregation for both groups of donors. Aggregation increased as the shear rate increased up to a maximum at $\bar{G}_{max}$ = 168 and 335 s^{-1} for male and female donors, respectively. Thereafter, aggregation decreased linearly with increasing shear rate down

TABLE 1 Average statistics of the single platelet log-volume distributions

Statistic	Male		Female	
	Log-normal	Not log-normal	Log-normal	Not log-normal
No. donors	35	12	25	17
HCT (%)	46.1 ± 2.2	44.9 ± 2.5	40.4 ± 2.5	40.1 ± 3.0
$\bar{\mu}$	7.3 ± 0.9	7.4 ± 1.1	7.3 ± 1.0	7.5 ± 1.1
σ	4.6 ± 0.8	4.7 ± 0.7	4.5 ± 0.9	4.7 ± 0.9
μ_{mod}	4.5 ± 0.5	4.5 ± 0.7	4.5 ± 0.4	4.5 ± 0.5
μ_{med}	6.2 ± 0.7	6.3 ± 0.9	6.3 ± 0.7	6.3 ± 0.9
g_1	0.014 ± 0.037	0.050 ± 0.112*	0.022 ± 0.046	0.086 ± 0.066‡
g_2	−0.035 ± 0.069	0.104 ± 0.154‡	0.002 ± 0.081	0.108 ± 0.098‡
$n_{L,U}(0)$	15385 ± 1313	15380 ± 1244	14904 ± 1269	15080 ± 1173

Statistics of individual platelet log-volume distributions calculated $\bar{t}$ = 0 s over the range 1–50 μm^3 averaged for the stated number of donors of each sex and further partitioned into those accepted as normal by the K-S one sample test and those rejected. Symbols are described in the text and volumes are in cubed micrometers. Significantly different from zero: *$P < 0.02$. ‡$P < 0.01$. ‡$P < 0.001$.

to a minimum at $\bar{G}$ = 1,000 and 1,335 s^{-1} for male and female donors, respectively. Further increases in shear rate, however, produced an increase in aggregation for both sexes. The two aggregation curves intersect at $\bar{G}$ = 1,335 s^{-1} where aggregation had begun to increase for the male donors while it was still decreasing for the female donors.

Although no significant aggregation was observed in the controls in which modified Tyrodes was infused, and no sex difference was present, there was a significant interaction ($P < 0.006$) between donor sex and mean tube shear rate as reflected by reciprocal changes in single platelet concentration. Thus, whereas there was breakup of preformed aggregates ($N_{1,30}[\bar{t}]/N_{1,30}[0] > 1$) for the males at $\bar{G}$ < 1,000 s^{-1}, there was a slight degree of aggregation ($0.93 < N_{1,30}[\bar{t}]/N_{1,30}[0] < 1$) of the platelets from the females. The opposite occurred at $\bar{G} > 1{,}000\ s^{-1}$. It is interesting that in the controls the single platelet concentrations for the male and female donors reversed at the same shear rate at which the ADP aggregation curves intersect.

The sex difference persisted through all mean transit times between $\bar{t}$ = 2.1 and 86 s. For the female donors at $\bar{G}_{max}$ = 335 s^{-1} only 13 ± 2.4% (n = 5) of single platelets remained unaggregated after $\bar{t}$ = 86 s, whereas for male donors after the same mean transit time, 37 ± 9.2% (n = 6) were unaggregated at $\bar{G}_{max}$ = 168 s^{-1}. Above $\bar{G}$ = 41.9 s^{-1}, the aggregation curves of both groups exhibited an initial time delay before the onset of significant aggregation. As discussed below, the length of this lag phase increased with increasing mean tube shear rate, and its effect was more pronounced for the female donors where changes in the single platelet concentration were greatest.

b. Donor hematocrit

A strong correlation of the normalized single platelet concentration with donor hematocrit (r = 0.91, $P <$ 0.001) was obtained when male and female donors at $\bar{t}$ = 43 s and $\bar{G}$ = 335 s^{-1} were grouped together. Similar, but generally less significant, correlations were found at all mean tube shear rates from 41.9 to 1,920 s^{-1}, except at $\bar{G}$ = 1,335 s^{-1} where no sex difference existed.

c. Thromboxane B_2

The concentration of TXB_2 was measured in PRP at $1{,}000 \le \bar{G} \le 1{,}920\ s^{-1}$ for several male and female donors. Although TXB_2 concentrations as high as 6 ng ml^{-1} in PRP and 10 ng ml^{-1} in PPP were obtained during platelet preparation, neither sex showed significant changes in TXB_2 concentration with time and shear rate from that at $\bar{t}$ = 0 s in either control or ADP infusion runs (Bell, 1988). Thromboxane B_2 concentration did not correlate with donor hematocrit in either PPP or in the PRP of the ADP infusion runs at $\bar{t}$ = 43 or 86 s, nor did it correlate with the normalized single platelet concentration at $\bar{G} \ge$ 1,335 s^{-1}.

3. Total particle concentration

a. Rate of aggregation

Mean values of the negative logarithm of the total particle concentration at time $\bar{t}$, $N_{1,10^5}(\bar{t})$, normalized to that at $\bar{t}$ = 0 s, $N_{1,10^5}(0)$, were plotted against $\bar{t}$ according to Eq. 12, part I, for the female donors in Fig. 2. Although the extent of aggregation was greatest at $\bar{G}$ = 335 s^{-1}, the highest rate of aggregation occurred within the first $\bar{t}$ = 2 s at $\bar{G}$ = 41.9 s^{-1} where the single platelet concentration decreased at a rate of 4.2% s^{-1} ± 0.9 (± SEM, n = 10). At this shear rate, the rate of aggregation steadily decreased with increasing mean transit time.

The combined effects of an initial lag phase followed by progressively increasing then decreasing rates of aggregation produced sigmoid aggregation curves for all $\bar{G} > 41.9$ s^{-1}. The length of the lag phase increased with increasing mean tube shear rate reaching $\bar{t} \sim$ 11 s at $\bar{G}$ = 1,335 s^{-1}. In addition, as the mean tube shear rate was raised, not only did the maximum rate of aggregation decrease, but it occurred at progressively increasing mean transit times. At $\bar{G}$ = 335 s^{-1} the maximum rate of aggregation of 2.8% s^{-1} ± 0.2 (n = 5) occurred between $\bar{t}$ = 8.6 and 21 s, whereas at $\bar{G}$ = 1,335 s^{-1} the rate was maximal at 1.0% s^{-1} ± 0.2 (n = 5) between $\bar{t}$ = 21 and 43 s. Male donors exhibited a pattern of aggregation similar to that of the female donors at the same shear rate but always with much longer lag phases and reduced rates of aggregation.

b. Collision efficiency

In addition to providing an index of the rate of aggregation, the slope of the curves in Fig. 2 can be used to calculate the collision efficiency according to Eq. 12, part I. The individual collision efficiencies of all donors at each mean tube shear rate were averaged over three time intervals for both sexes, as shown in Table 2. A maximum collision efficiency, α_0 = 0.264, was obtained at $\bar{G}$ = 41.9 s^{-1} between $\bar{t}$ = 0 and 4.3 s. Throughout all three time intervals, α_0 either decreased or remained constant as the mean tube shear rate was increased up to $\bar{G}$ = 1,335 s^{-1} where $\alpha_0 \le 0.002$. At $\bar{G}$ = 1,920 s^{-1}, there was a small but significant increase in collision efficiency which, together with the high collision frequency, was sufficient to support a high rate of aggregation (Fig. 1).

The dependence of collision efficiency on time and shear rate is revealed in Fig. 3 in a plot of α_0 against $\log \bar{t}\bar{G}$ for each of the time intervals listed in Table 2 for

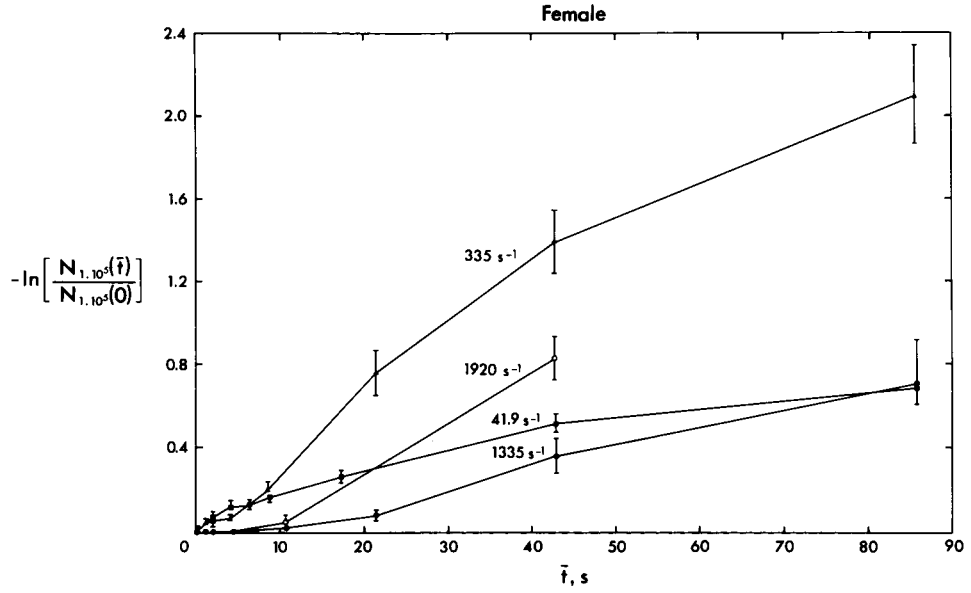

FIGURE 2 Total particle concentration. The negative logarithm of the normalized, total particle concentration, $-\ln [N_{1,10^5}(\bar{t})/N_{1,10^5}(0)]$, (±SEM) plotted against $\bar{t}$ and $\bar{G}$ = 41.9, 335, 1,335, and 1,920 s^{-1} for the female donors.

the female donors. In the time interval from $\bar{t}$ = 0–4.3 s, both the collision efficiency and its rate of decrease fell rapidly with increasing $\bar{G}$. A similar decline in α_0 in the interval from $\bar{t}$ = 4.3 to 8.6 s was interrupted between $\bar{G}$ = 168 and 335 s^{-1} before resuming at a higher rate of decrease beyond $\bar{G}$ = 335 s^{-1}. In contrast, during the time interval from $\bar{t}$ = 8.6–21 s, α_0 decreased by only 12% up to $\bar{G}$ = 168 s^{-1}, but decreased sharply thereafter.

A similar pattern was observed for the collision efficiencies from male donors, although the two-phase decrease in α_0 between $\bar{t}$ = 4.3 and 8.6 s was less pronounced.

TABLE 2 Effect of shear rate and transit time on collision efficiency

Sex	$\bar{G}$	$\alpha_0 \times 10^3$ (± SEM)		
		$\bar{t}$ = 0–4.3 s	4.3–8.6 s	8.6–21 s
	s^{-1}			
Male	41.9	118 ± 30.0	68.0 ± 21.5	59.0 ± 14.6
	168	19.9 ± 10.3	25.5 ± 8.2	49.1 ± 11.5
	335	7.51 ± 2.46	13.9 ± 4.4	22.3 ± 3.1
	1335	2.27 ± 0.79	0.93 ± 0.38	1.92 ± 0.43
	1920	1.98 ± 0.68	1.65 ± 0.47	—
Female	41.9	264 ± 64.8	88.2 ± 28.6	108 ± 20.5
	168	38.2 ± 7.1	35.2 ± 9.8	94.7 ± 18.8
	335	17.4 ± 4.9	35.3 ± 8.2	49.9 ± 7.6
	1335	0.01 ± 0.01	1.80 ± 0.54	2.01 ± 0.67
	1920	0.62 ± 0.34	2.30 ± 0.89	—

[ADP] = 0.2 μM.

4. Aggregate growth

a. Aggregate size distribution

The evolving pattern of aggregate growth for the female donors is illustrated in Figs. 4–6 through plots of the normalized average class volume fraction $\bar{\Phi}(x_i)$, versus particle volume at successive mean transit times. The decrease in single platelet concentration (1–30 μm^3) was accompanied by a sequential rise and fall of aggregates of successively increasing volume. The steadily decreasing rate of aggregation with time shown earlier (Fig. 2) at $\bar{G}$ = 41.9 s^{-1} was associated with the formation of aggregates having a broad spectrum of size at $\bar{t}$ = 86 s (Fig. 4). At $\bar{G}$ = 335 s^{-1} (Fig. 5), no distinct aggregate peaks were present before $\bar{t}$ = 8.6 s, but by $\bar{t}$ = 21 s aggregates of relatively discrete size had appeared. As aggregation continued, the upper limit of aggregate size increased. By $\bar{t}$ = 86 s, most aggregates were present in one large group, a significant proportion of which exceeded 10^5 μm^3, the largest volume measured. Although there was considerable aggregation at $\bar{G}$ = 1,920 s^{-1} (Fig. 6), the aggregates were smaller and occupied a size range considerably narrower than at the same mean transit time at $\bar{G}$ = 335 s^{-1}. A similar pattern of aggregate growth was exhibited by the male donors; however, aggregate size was always much reduced compared to that for the female donors at the same mean transit time and mean tube shear rate.

2. Aggregate growth rate

Figs. 4–6 illustrate the continuity in the evolving distribution of aggregate size, but they do not convey a sense of

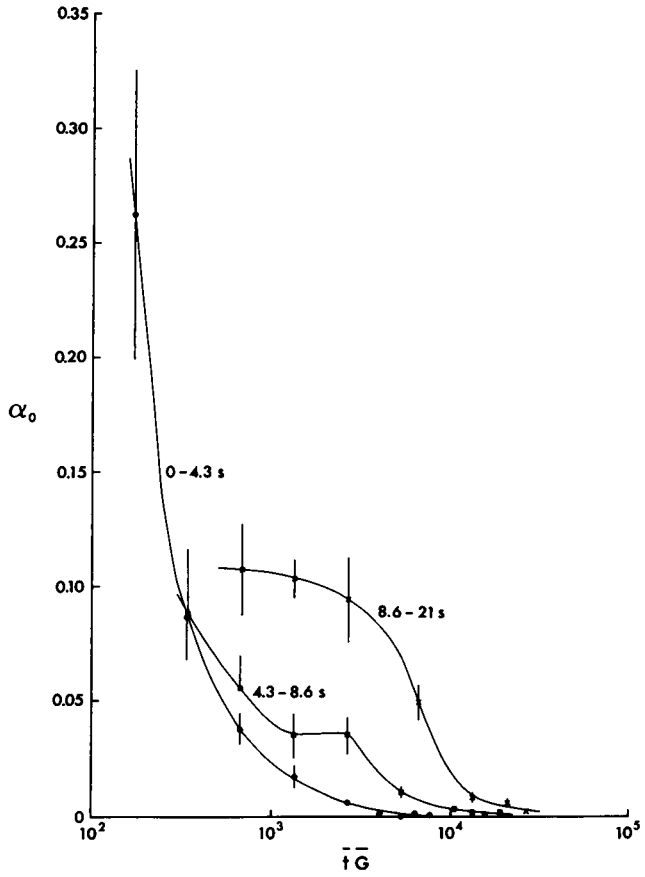

FIGURE 3 Collision efficiency, α_0, (±SEM) over three time intervals, $\bar{t}$ = 0–4.3, 4.3–8.6, and 8.6–21 s plotted against $\bar{t}\bar{G}$. Data from the female donors previously shown in Fig. 2.

the rate of aggregate growth. This is provided in Fig. 7 where the volume fraction of aggregates, $\Phi_{L,U}(\bar{t})$, between lower, L, and upper, U, volume limits was normalized to the total volume fraction $\Phi_{1,10^5}(0)$, at $\bar{t}$ = 0 s. As previously noted, small aggregates were present at $\bar{t}$ = 0 s. At $\bar{G}$ = 41.9 s^{-1}, a rapid rise in the volume fraction of aggregates from 30 to 10^2 μm^3 was followed by increases in the volume fraction of aggregates of successively increasing size. At higher shear rates, changes in the volume fraction of single platelets (L = 1, U = 30) with increasing mean transit time followed the same sigmoid curve as did changes in the single platelet and total particle number concentration described previously. The sequential formation of aggregates of discrete size and their subsequent incorporation into aggregates of larger size were clearly evident. The total normalized volume fraction exceeded 1.0 with the appearance of aggregates $>10^3$ μm^3, but decreased again as the number of aggregates $>10^4$ μm^3 increased. The lag phase preceding aggregation was evident through delays in the onset of changes in the volume fraction of both single cells and aggregates. The lag phase increased with increasing mean tube shear rate up to $\bar{G}$ = 1,335 s^{-1} where no aggregates $>10^4$ μm^3 were formed. Even though the lag phase at $\bar{G}$ = 1,920 s^{-1} was shorter and the rate of aggregation higher than at $\bar{G}$ = 1,335 s^{-1}, the aggregates formed were still smaller than those at $\bar{G}$ = 335 s^{-1} at the same mean transit time.

Male donors had consistently longer lag phases and lower rates of aggregation than female donors. In addition, there was a significant difference in the pattern of aggregate growth at $\bar{G}$ = 335 s^{-1}. The volume fraction of the largest aggregates measured at $\bar{t}$ = 43 s (10^4–10^5 μm^3)

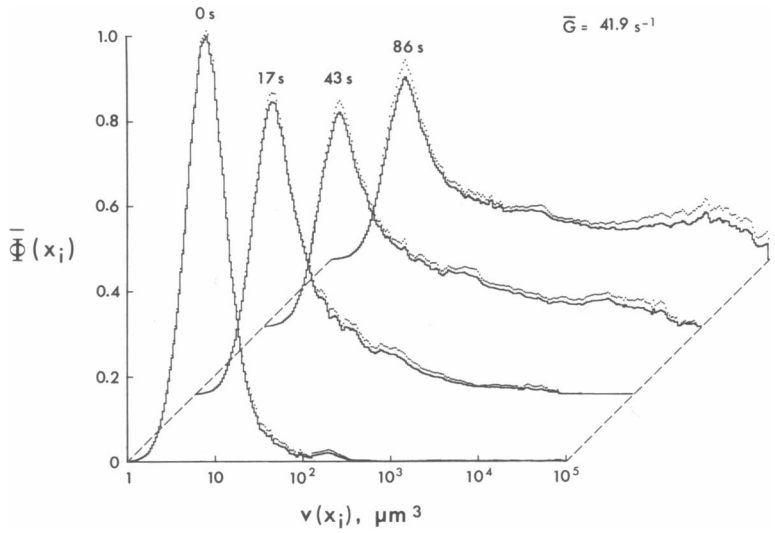

FIGURE 4 Volume fraction histograms at $\bar{G}$ = 41.9 s^{-1}. Three-dimensional plot of the mean, normalized class volume fraction $\bar{\Phi}(x_i)$, (±SEM, *dotted line*) vs. particle volume at mean transit times from $\bar{t}$ = 0–86 s for the female donors at $\bar{G}$ = 41.9 s^{-1}. The time axis (*dashed line*) is not drawn to scale.

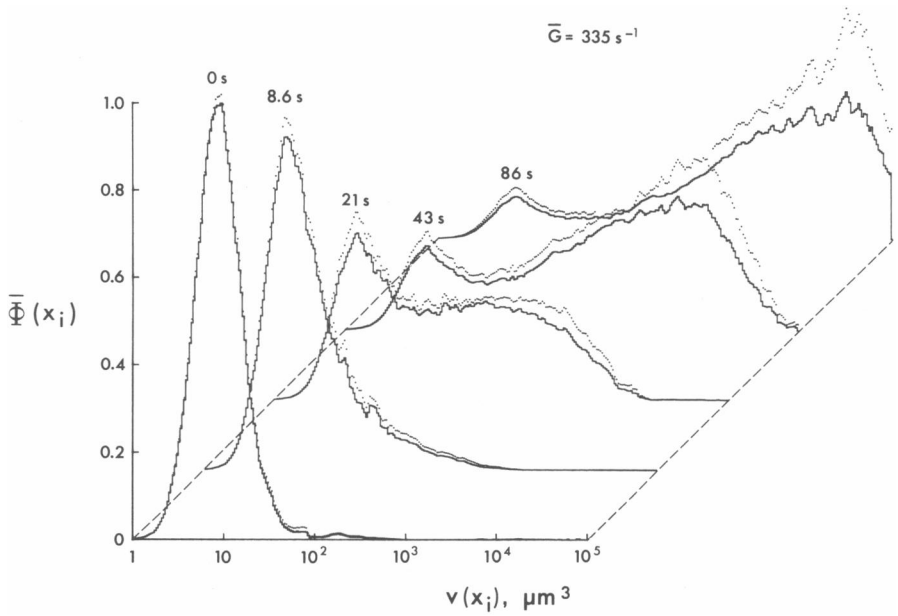

FIGURE 5 Volume fraction histograms at $\bar{G}$ = 335 s^{-1}. Plot as in Fig. 4 for the female donors.

was greater than that of aggregates in the next smallest group (10^3–10^4 μm^3). The concentration of the largest aggregates subsequently decreased at $\bar{t}$ = 86 s; however, that of aggregates from 10^2–10^3 μm^3 and 10^3–10^4 μm^3 continued to increase, and the latter at a greater rate. This phenomenon is indicative of aggregate breakup at long transit time.

5. ADP concentration

a. Single platelet concentration

Platelet-rich plasma from single representative male and female donors of widely different hematocrit (HCT = 43.9 and 34.5%, respectively) was sheared at $\bar{G}$ = 41.9, 335, and 1,920 s^{-1} in the presence of 0.2 and 1.0

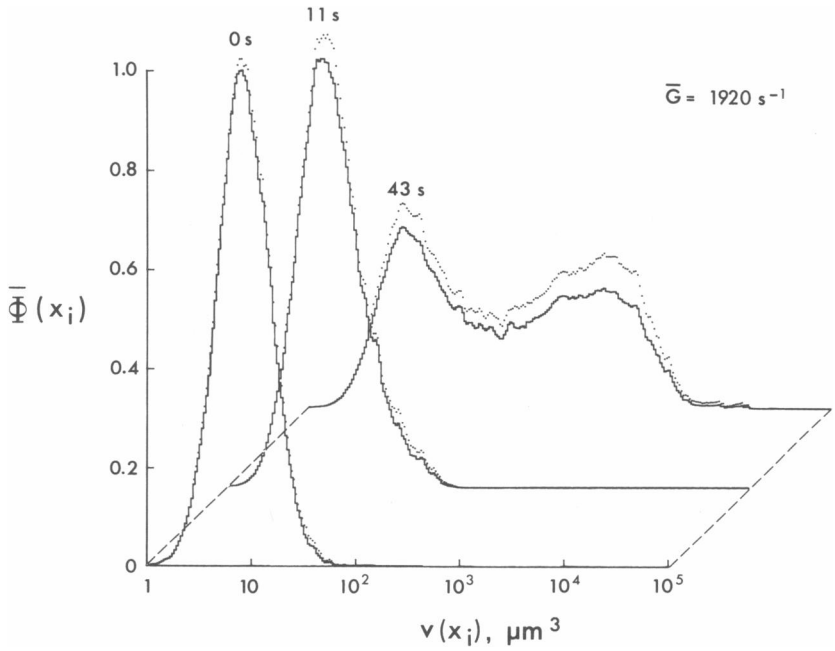

FIGURE 6 Volume fraction histograms at $\bar{G}$ = 1,920 s^{-1}. Plot as in Figs. 4 and 5 for the female donors.

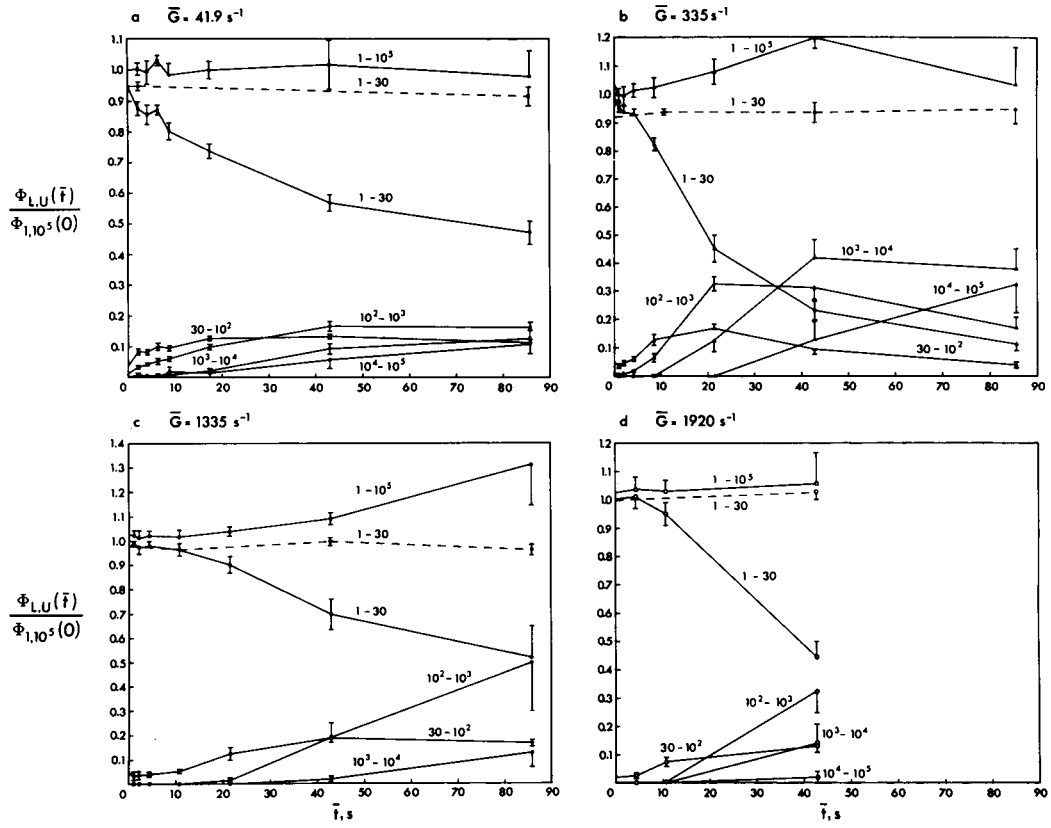

FIGURE 7 Effect of shear rate on aggregate growth for females. The normalized volume fraction of particles between lower, L, and upper, U, volumes $\Phi_{L,U}(\bar{t})/\Phi_{1,10^5}(0)$ (±SEM), plotted against $\bar{t}$ for the female donors. The volume limits, L-U, from 1–30, 30–10^2, 10^2–10^3, 10^3–10^4, 10^4–10^5, and 1–10^5 μm^3 are shown beside their respective plots. No particles were present in volume ranges not listed. Dashed line represents the control values of single platelets (1–30 μm^3).

μM ADP. At equivalent mean transit times and mean tube shear rates, the extent of aggregation was always greater at 1.0 μM ADP than at 0.2 μM ADP for both the male and the female donor. As previously found at 0.2 μM ADP, aggregation was greater for the female donor than for the male donor at all shear rates and transit times with the greatest difference at $\bar{G}$ = 335 s^{-1}. At this shear rate aggregation was minimal before $\bar{t}$ = 4.3 s. At 1.0 μM ADP, however, the male donor exhibited a degree of aggregation greater than that of the female donor at $\bar{G}$ = 41.9 and 335 s^{-1}, while both donors exhibited the greatest aggregation at $\bar{G}$ = 1,920 s^{-1} with no apparent sex difference. It is interesting that at this shear rate <1% of single platelets remained unaggregated at $\bar{t}$ = 43 s.

b. Collision efficiency

Values of the collision efficiency at 0.2 μM ADP for the female donor (Table 3) were consistent with the mean values of the female donors given in Table 2, whereas those for the male donor showed more variation, particularly at $\bar{G}$ = 41.9 s^{-1} where they were considerably higher.

TABLE 3 Effect of ADP concentration on collision efficiency and rate of aggregation

Sex	ADP	TXB_2*	$\bar{G}$	$\bar{t}$ = 0–4.3 s		4.3–11 s	
				α_0‡	Rate§	α_0‡	Rate§
	μM	$ng\ ml^{-1}$	s^{-1}	$\times 10^3$	$\%\ s^{-1}$	$\times 10^3$	$\%s^{-1}$
Male	0.2	1.35	41.9	260	2.2	73.8	0.6
		0.78	335	0.00	0.0	21.9	1.7
		0.50	1920	0.96	0.4	3.19	1.3
	1.0	2.28	41.9	717	5.7	223	1.3
		0.99	335	46.7	3.2	205	8.1
		0.72	1920	5.11	2.0	41.4	9.5
Female	0.2	0.52	41.9	313	3.0	78.5	0.8
		0.41	335	25.9	2.1	36.3	2.6
		0.76	1920	0.37	0.3	4.65	2.0
	1.0	0.27	41.9	231	2.6	131	1.0
		0.26	335	24.7	2.1	55.2	3.7
		0.65	1920	9.4	4.2	34.5	8.4

*Measured at $\bar{t}$ = 43 s. ‡Calculated from Eq. 12, part I. §Given as percent decrease in normalized single platelet concentration.

At 1.0 μM ADP there was a large increase in α_0 at all mean transit times and mean tube shear rates. A notable exception was at $\bar{G}$ = 41.9 s^{-1} between $\bar{t}$ = 0 and 4.3 s for the female donor, where α_0 actually decreased. For the male donor at this shear rate and time interval, however, the collision efficiency increased dramatically from α_0 = 0.260 to 0.717.

As previously found at 0.2 μM ADP (Table 2), at all mean transit times with both 0.2 and 1.0 μM ADP, α_0 decreased with increasing mean tube shear rate. Collision efficiency also decreased with increasing mean transit time at $\bar{G}$ = 41.9 s^{-1}, but increased with $\bar{t}$ at the higher shear rates. The concentration of TXB_2 at $\bar{t}$ = 43 s was generally <1.0 ng ml^{-1} at all shear rates with either ADP concentration for both donors (Bell, 1988).

c. Rate of aggregation

Table 3 also shows the rate of decrease of the normalized single platelet concentration over the same time interval that the two-body collision efficiency was calculated. At 0.2 μM ADP the rates of aggregation of platelets from the female donor were generally greater than those from the male donor at all mean tube shear rates and mean transit times, with maximum values for both donors at $\bar{G}$ = 41.9 s^{-1} between $\bar{t}$ = 0 and 4.3 s. As previously found at this $\bar{G}$, longer transit times resulted in decreased rates of aggregation, but as the shear rate was increased the maximum rates of aggregation both decreased and occurred at progressively longer transit times.

A similar pattern was observed with 1.0 μM ADP at $\bar{G}$ = 41.9 and 335 s^{-1} with the maximum rates of aggregation being generally greater than those at 0.2 μM ADP. This was particularly true for the male donor where the rates of aggregation now exceeded those for the female donor. The highest rate of aggregation also shifted to $\bar{G}$ = 1,920 s^{-1} between $\bar{t}$ = 4.3 and 11 s where the single platelet concentration decreased at rates of 9.5 and 8.4% s^{-1} for the male and female donor, respectively.

d. Aggregate growth

Aggregate growth between $\bar{t}$ = 0 and 43 s is shown as a function of ADP concentration for the female donor at $\bar{G}$ = 335 and 1,920 s^{-1} in Fig. 8. At 0.2 μM ADP, the pattern of growth was typical of that shown in Figs. 5 and 6. At 1 μM ADP, the much greater rate of aggregation at the same shear rates led to the production of larger aggregates. At $\bar{G}$ = 1,920 s^{-1}, the aggregates were unusually tightly grouped into a single population between 10^4 and 10^5 μm^3 with no larger or smaller aggregates, and virtually no single platelets remaining. An increase in the overall volume fraction of these aggregates is seen by the magnitude of the ordinate of these log-volume distributions. The small population of particles between 130 and 260 μm^3 at $\bar{t}$ = 0 and 43 s are

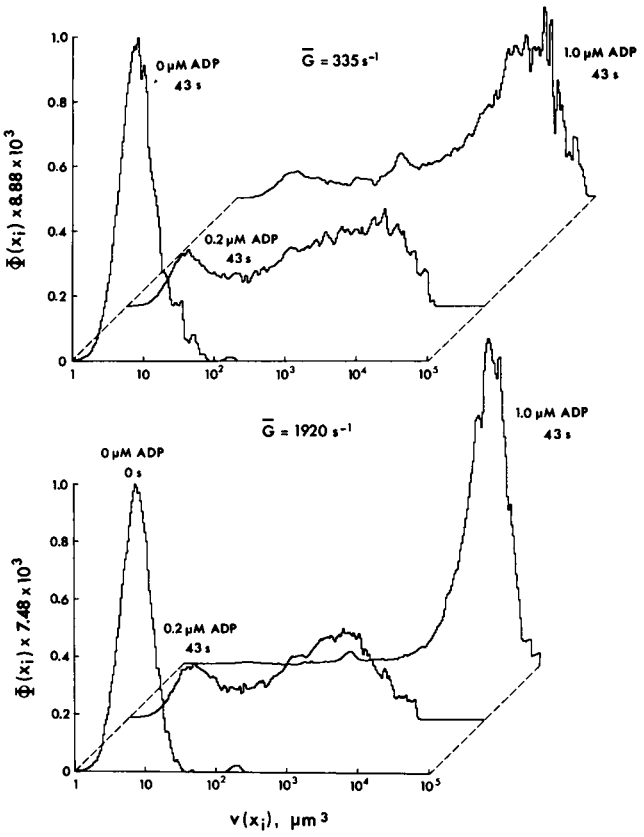

FIGURE 8 Aggregate growth vs. [ADP] at $\bar{G}$ = 335 and 1,920 s^{-1} for a female donor. Three dimensional plot of the volume fraction per histogram class, $\Phi(x_i)$, vs. particle volume, $v(x_i)$ after $\bar{t}$ = 43 s exposure to 0.2 and 1.0 μM ADP. Also shown is a control at $\bar{t}$ = 0 s.

white cells which were not incorporated into aggregates. At 0.2 μM ADP, both the number and size of aggregates of platelets from the female donor were greater than those from the male donor (not shown), whereas the single platelet concentration was, accordingly, much reduced. The sex difference was most pronounced at $\bar{G}$ = 335 s^{-1}. At 1 μM ADP, however, no sex difference was apparent.

DISCUSSION

The present work is the first account of the ADP-induced aggregation of human platelets in Poiseuille flow to span the full range of physiologically significant shear rate. Within this range, the rate of single platelet aggregation and the rate of aggregate growth were both highly dependent on mean transit time and mean tube shear rate. An increase in the lag phase preceding aggregation with increasing shear rate suggests a latency in the expression of platelet–platelet bonds of high strength. Measurement of the two-body collision efficiency also

suggests the presence of more than one type of platelet–platelet bond. In addition, a strong sex difference was observed in both the rate of single platelet aggregation and size of aggregates.

1. Platelet size

The log-normal model for the distribution of platelet size (Bahr and Zeitler, 1965; Paulus, 1975; von Behrens, 1972) was verified independently for platelet volume from male and female donors. The average mean platelet volume of 7.3 μm^3, uncorrected for platelet shape, is consistent with previous uncorrected measurements of mean platelet volume obtained using electronic particle counters (Holme and Murphy, 1980; Mundschenk et al., 1976; Paulus, 1975). Paulus (1975) has proposed that the log-normal size distribution of platelets is a consequence of random factors controlling the combined rates of growth and demarcation of platelet territories during megakaryocyte maturation. Megakaryocyte polyploidy and platelet aging in the circulation have also been postulated as a source of platelet heterogeneity (Corash et al., 1978; Karpatkin, 1969*a* and *b*; Pennington et al., 1976; Rand et al., 1981).

The Kolmogorov-Smirnov one sample test was sensitive to small departures from log-normality and was supported by significant changes in the shape of the log-volume distributions as measured by the statistics of skewing and kurtosis. Those distributions accepted by the K-S test as log-normal did not exhibit skewing or kurtosis. Those distributions rejected by the K-S test, however, were both significantly positively skewed and leptokurtotic, i.e., more platelets were located at the mean and extreme log-volumes than at intermediate values. Taken together, these parameters point to the presence of contaminating microaggregates that were formed during platelet preparation. The presence of preformed microaggregates is also revealed by their subsequent breakup in the controls, and at early times at $\bar{G} \geq 670\ s^{-1}$ in the ADP infusion runs.

2. Application of two-body collision theory

Theory, applicable to inert, charged colloidal-size particles, predicts that when net attractive forces operate between colliding particles, the two-body collision efficiency decreases with increasing shear stress (van de Ven and Mason, 1977). This has been shown experimentally at shear stresses $<0.2\ Nm^{-2}$ for the aggregation of model latex spheres in solutions of high ionic strength (Curtis and Hocking, 1970; Swift and Friedlander, 1964; Zeichner and Schowalter, 1977) and human platelets exposed to 1 μM ADP (Bell and Goldsmith, 1984). In the present experiments the mean tube shear stress, $\tau = \eta\bar{G}$, ranged from 0.08 to 3.5 Nm^{-2} (η = 1.8 mPa s). As the mean tube shear rate increases, the extent of aggregation is the result of a balance between an increased frequency of collision (Eq. 10, part I) and an increased fluid shear stress. High collision rates support a high rate of aggregation in the absence of shear stresses sufficient to inhibit doublet formation. Beyond an optimum shear rate for aggregation, higher fluid shear stresses can prevent stable platelet–platelet bond formation and aggregation decreases. Short interaction times may limit stable doublet formation at high shear rates but, because this time is inversely proportional to the shear rate, it is impossible to separate the effects of short interaction time and high shear stress in limiting stable bond formation. The two-body collision efficiency, however, takes both effects into account by measuring the fraction of total platelet–platelet collisions that result in stable doublet formation.

The collision efficiencies given in Tables 2 and 3 were computed from changes in the total particle concentration using Eq. 12, part I, which assumes that the decrease in total particle concentration with time is due only to the formation of doublets. This assumption can be tested by calculating the fraction of successful two-body collisions from the initial rate of single platelet decrease. The total number of two-body collisions per unit volume of suspension per second can be calculated from Eq. 10, part I, using the initial number concentration and volume fraction of single platelets:

$$J = \frac{4\Phi_{1,30}(0)\, N_{1,30}(0)\, \bar{G}}{\pi}. \quad (1)$$

If α_0 computed from the total particle concentration is significantly greater than that computed using Eq. 1, then higher order aggregates are present in appreciable numbers. At 0.2 μM ADP and $\bar{G} = 41.9\ s^{-1}$, where the mean volume fraction of single platelets was 0.195 ± 0.023% (±SD) for male donors and 0.197 ± 0.023% for female donors, respective initial rates of single platelet decrease of 2.7 and 4.2% s^{-1} yielded collision efficiencies of 0.14 and 0.21. These values are remarkably similar to the collision efficiencies, 0.12 and 0.26, calculated according to Eq. 12, part I, between $\bar{t}$ = 0 and 4.3 s (Table 2), well into the aggregation reaction. Actually, one would expect the collision efficiency calculated at long times to yield lower values due to the decrease in particle concentration with increasing aggregation. Thus, it is unlikely that the observed increase in collision efficiency with time in the present experiment is artifactual. It should be noted, however, that the presence of pseudopods on the activated platelets has been estimated to double the effective collision diameter of the cells (Frojmovic and Longmire, 1986). This will result in an eightfold increase in collision frequency and a corresponding decrease in α_0, and implies

that the aggregation reaction is capable of propagation at very low collision efficiencies.

3. Effect of shear rate

ADP concentrations of 0.2 and 1.0 μM were selected to give consistently the same respective patterns of aggregation in the aggregometer as 1 and 5–10 μM ADP at 37°C, within the natural variation among donors. Thus, platelet aggregation at 22°C was about five times greater than at 37°C; however, the release reaction was inhibited (Bell, 1988). Release could only be induced in the aggregometer at 22°C by high concentrations of thrombin. This is in agreement with Valdorf-Hansen and Zucker (1971) who showed the release of platelet serotonin induced by ADP but not thrombin to be inhibited below 27°C. Shear stresses of 15 Nm^{-2} are required to induce platelet granule release at room temperature within exposure times of the present experiments (Hellums and Hardwick, 1981). In the present work, wall shear stresses reached 6.5 Nm^{-2}, and thromboxane A_2 (TXA_2), as measured by the stable end-product TXB_2, was not significantly higher than in static controls at mean tube shear rates between 41.9 and 1,920 s^{-1} in either the control runs or with 0.2 and 1.0 μM ADP. Furthermore, there was no shear-induced aggregation in the controls at the same level of shear stress. Thus, neither shear-induced platelet aggregation nor ADP- or shear-induced platelet release are likely to have contributed to the observed aggregation. It is possible, however, that platelet surface activation in concert with ADP stimulation led to the enhanced affinity of existing receptors, the exposure of latent receptors or the induction of some independent mechanism of aggregation (discussed later). In the discussion to follow, 0.2 and 1.0 μM ADP are referred to as low and high platelet stimulation, respectively.

a. Low platelet stimulation

i. Single platelet aggregation. Neglecting for the moment the sex difference, the extent of platelet aggregation increases with increasing mean tube shear rate up to an optimum value at ~335 s^{-1}. Higher shear rates result in a steady decline in aggregation which increases again beyond 1,335 s^{-1}. It is interesting that the highest rate of aggregation was at the lowest shear rate but this was true for only the first few seconds of aggregation. The two-body collision efficiency was also highest under these conditions. Even so, at most only 26% of all collisions resulted in stable doublet formation. Although the fluid shear stress is low, the collision rate is not sufficient to sustain a high rate of aggregation. At higher shear rates there was generally a decrease in the fraction of efficient collisions but a high collision frequency accounts for the higher rates of aggregation. At the maximum shear rate in the present experiments, collision efficiencies between 0.6×10^{-3} and 2.3×10^{-3} were measured. This is in good agreement with the values reported for shear-induced platelet aggregation at shear rates between 2,000 and 10,000 s^{-1} (Belval and Hellums, 1986). Thus, the collision efficiency, which decreases by approximately two orders of magnitude between $\bar{G}$ = 41.9 and 1,335 s^{-1}, remains relatively constant thereafter up to shear rates of 10,000 s^{-1}. The large decrease in collision efficiency at relatively low shear rates (Table 2) and the persistence of a nonzero collision efficiency at high shear rates suggest that more than one type of platelet–platelet bond mediates ADP-induced aggregation.

The increasing rates of aggregation with time as depicted by the sigmoid aggregation curves (Figs. 2 and 7) indicate that collision efficiency increases with time, even after a delay of up to 11 s in the onset of aggregation. Indeed, not only do calculations of collision efficiency confirm this but they also indicate that the heterogeneity among platelet bonds is time-dependent (Fig. 3). At early transit times the high rate of aggregation at low shear rates is sustained by a weak bond that is easily disrupted at higher shear rates resulting in a corresponding shear-dependent lag phase. Even at low shear rates the strength of this bond gradually diminishes with increasing transit time and, in conjunction with a low collision rate, produces a steadily decreasing rate of aggregation. At high shear rates, the increasing rate of aggregation at times beyond the lag phase reveals the emergence of a second stronger bond. Longer times are required before each bond is sufficiently strong, or is present in sufficient numbers, to support aggregation. The two types of bonds coexist at intermediate transit times where the weak bond is disrupted at low shear rates but higher shear rates are required to disrupt the stronger bonds. The interruption in the decrease in collision efficiency with increasing mean tube shear rate between 168 and 335 s^{-1} at mean transit times between 4.3 and 8.6 s (Fig. 3) points to a transition from weak to strong bond. At very long exposure times the strong bonds are maximally expressed through either strength or numbers, and only high shear rates are sufficient to disrupt them.

ii. Mechanisms of ADP-induced platelet aggregation. The cross-linking of bivalent fibrinogen molecules between activated glycoprotein IIb-IIIa (GPIIb-IIIa) complexes in the platelet membrane is the mechanism believed to underlie the ADP-induced aggregation of platelets (Leung and Nachman, 1986). The steadily increasing lag phase preceding aggregation with increasing shear rate in the present work points to a latency in the strength of the platelet–platelet cross-bridge. An argument can be made for the requirement of latency in the

expression of platelet bonds from the limitations placed on any colloid whose aggregation is mediated by polymer cross-linking. For cross-linking to occur, unoccupied binding sites must be available on both surfaces. In the case of platelets, the high concentration of fibrinogen in plasma would be expected to saturate all binding sites on platelets before cross-linking could occur. In fact, cross-linking would require the simultaneous binding of opposite ends of the bivalent fibrinogen molecule to two platelets immediately after activation of GPIIb-IIIa complexes, and before saturation of these receptors with free fibrinogen. This scenario seems unlikely given the high concentration of fibrinogen in plasma ($\sim 2 \times 10^7$ molecules per platelet). It is more likely that all GPIIb-IIIa complexes ($\sim 5 \times 10^4$ receptor sites per cell; Nurden, 1987) would be saturated with free fibrinogen long before two platelets could simultaneously bind a single fibrinogen molecule. Instead, a model of aggregation requires either a low affinity for fibrinogen binding by activated platelets, and the subsequent continuous breaking and forming of new platelet-fibrinogen bonds, or the time-dependent exposure of new bonds that permits cross-linking during the interaction time of collision. Peerschke et al. (1980) have provided evidence for both high and low affinity binding sites for ^{125}I-labeled fibrinogen on ADP stimulated platelets; however, Marguerie et al. (1980) found only a single class of receptors. In both cases binding was saturable and required the continuous presence of ADP in the absence of release. Both groups reported that binding increased with time; however, Peerschke et al. found binding to reach equilibrium after 1 min, whereas Marguerie et al. measured increased binding up to 30 min. In addition, fibrinogen itself appears to have a binding sequence in the carboxy terminus of the γ-chain that recognizes the GPIIb-IIIa complex, but is distinct from the arginine-glycine-aspartic acid (RGD)–containing sequence in the α chain (Kloczewiak et al., 1984; Santoro and Lawing, 1987). Thus, the relatively slow kinetics of fibrinogen binding and the existence of heterogeneity in the affinity of fibrinogen provide a mechanism for platelet aggregation in the presence of high concentrations of the cross-linking ligand. Furthermore, the increase in the two-body collision efficiency with time and the formation of a high shear rate-resistant bond can be explained in terms of a time-dependent increase in fibrinogen binding.

Evidence for fibrinogen binding comes from the covalent cross-linking of fibrinogen to the GPIIb-IIIa complex (Bennett et al., 1982), and by the inhibition of binding by RGD-containing peptides (Gartner and Bennett, 1985; Haverstick et al., 1985; Plow et al., 1985) and by monoclonal antibodies that recognize the GPIIb-IIIa complex (Bennett et al., 1983; Coller et al., 1983). These binding assays do not prove, however, that fibrinogen mediates aggregation by directly cross-linking activated platelets. It has been proposed that GPIIb-IIIa receptor clustering is a prerequisite for fibrinogen binding and platelet aggregation (Aasch et al., 1985; Newman et al., 1987). It is possible that the role of fibrinogen is to stabilize such clusters permitting them to interact in some complementary manner between activated platelets. Thus, fibrinogen cross-linking between platelets per se would not be necessary for aggregation. If the platelets were initially aggregated by a mechanism independent of fibrinogen cross-linking but which maintained close contact, cross-linking could follow as fibrinogen-binding sites were expressed. Coller (1983) has proposed that both platelet binding of fibrinogen and the small radius of curvature of the pseudopods would be sufficient to lower the electrostatic repulsion between the similarly charged platelets and permit aggregation through van der Waals attraction. Because such aggregation is not mediated by specific fibrinogen cross-linking, it may not be resistant to high shear rates. It does, however, provide a mechanism for the relatively weak aggregation observed at short transit times in the present work.

Recent studies suggest that GPIIb-IIIa is involved in both platelet adhesion and aggregation onto subendothelium (Sakariassen et al., 1986; Weiss et al., 1986), and that von Willebrand Factor (vWF) is the principal ligand involved (Weiss et al., 1989). Moreover, vWF has been found to substitute for fibrinogen in the ADP-induced aggregation of washed platelets (Timmons and Hawiger, 1986) and of platelets from patients with afibrinogenemia (De Marco et al., 1986). Work on shear-induced platelet aggregation has also shown that vWF appears to mediate platelet aggregation in suspension at high shear rates at exposure times of 30 s and that high molecular weight forms, such as found in the α-granules of platelets, are the most effective (Moake et al., 1986; Moake et al., 1988). However, in the absence of significant release of vWF from the α-granules, plasma vWF can successfully mediate platelet aggregation. Both membrane glycoproteins GPIb and GPIIb-IIIa appeared to be essential for the vWF-mediated aggregation, as was activation of the surface receptors by endogenous ADP released from platelets at shear stresses between 3 and 6 Nm^{-2}. It is therefore possible that plasma vWF binding is responsible for the high shear rate–resistant bond in the present work. Although there was no release, platelet activation by ADP may have been sufficient to induce vWF binding.

iii. Aggregate size. The wide spectrum of aggregate size at $\bar{G} = 41.9\ s^{-1}$ shows that aggregate growth is not limited by a shear stress of 0.08 Nm^{-2}. Although the fluid shear stress is low, the collision rate is not sufficient to sustain a high rate of aggregation and the subsequent "snowball" effect found previously at this shear rate with

1 μM ADP (Bell and Goldsmith, 1984). In the present work this effect was evident at $\bar{G} = 335\ s^{-1}$, where large numbers of small aggregates that rapidly accumulated were subsequently incorporated into a new relatively homogeneous population of larger aggregates. Analysis of aggregate size distributions has shown similar behavior for aggregation induced by ADP in the aggregometer (Nichols and Bosmann, 1979) or by shear rates >2,000 s^{-1} in rotational viscometers (Belval and Hellums, 1986; Belval et al., 1984). This form of aggregate growth is characteristic of the successive rise and fall in the number of small order multiplets of progressively increasing size predicted by Smoluchowski (1917) for model spheres and verified experimentally for platelets at $\bar{G} \leq 54\ s^{-1}$ (Bell and Goldsmith, 1984). The sequential formation of similarly sized aggregates of relatively large size in the present experiments may have been encouraged by the presence of a limiting shear rate that restricts aggregate size at each mean transit time. The effect of this limit is more pronounced at $\bar{G} = 1{,}920\ s^{-1}$ where despite a high rate of aggregation, aggregate size was much reduced compared to that at $\bar{G} = 335\ s^{-1}$. It is known that for particle aggregation in the presence of adsorbed polymer, aggregates of equal-sized particles are more readily broken up than aggregates of unequal-sized particles by shear stresses capable of disrupting polymer bonds (van de Ven, 1982). Because fibrinogen cross-linking between activated platelets is analogous to polymer bridging, this effect would favor the aggregation of single platelets and aggregates at high shear rates.

b. High platelet stimulation

Comparison of the rate of single platelet aggregation for the two donors tested shows a slight shear-dependent lag phase still present. In spite of a threefold increase in the collision efficiency at $\bar{G} = 41.9\ s^{-1}$ for the male donor, the collision rate still could not support massive aggregation (Bell, 1988). Aggregate size was only slightly greater than at 0.2 μM ADP. The high collision efficiency may reflect a large increase in the affinity or number of fibrinogen-binding sites at the higher level of platelet stimulation. An increase in the length or numbers of platelet pseudopods may also increase the effective collision cross-section of the cells. This effect may be responsible for collision efficiencies greater than unity that have been measured for ADP-induced platelet aggregation due to Brownian motion (Frojmovic and Longmire, 1986). The opposite effects of a high collision efficiency and a size-dependent limiting shear rate are strikingly evident at high shear rates. At $\bar{G} = 335\ s^{-1}$ there was a large increase in both the rate of single platelet aggregation and aggregate size. The high rate of decrease in the single platelet concentration at $\bar{G} = 1{,}920\ s^{-1}$ between 4.3 and 11 s of 8–10% s^{-1} led to the rapid depletion of virtually all single platelets; however, aggregate growth was severely limited. The aggregates were grouped into a narrow volume distribution between 10^4 and 10^5 μm^3, yet at $\bar{G} = 335\ s^{-1}$ where many single platelets still remained, aggregate volume greatly exceeded 10^5 μm^3. The mean shear stress of 3.5 Nm^{-2} did not inhibit the recruitment of all platelets into aggregates but clearly did inhibit aggregate growth.

It has been suggested that some platelets within a normal population typically do not aggregate (Born and Hume, 1967; Gear, 1982; Nichols and Bosmann, 1979). The present work shows clearly that given a sufficient collision frequency and degree of platelet activation all platelets will aggregate. Neglecting the overlap of single platelet and microaggregate volume, the shape of the single platelet log-volume distribution remained symmetrical about the initial modal volume during aggregation indicating that all single platelets were being recruited equally well into aggregates. Belval et al. (1984) also observed the aggregation of almost the entire single platelet population as a result of shear-induced aggregation at shear rates >3,000 s^{-1}.

4. Sex difference

There is a highly significant sex difference in the aggregation of human platelets in response to 0.2 μM ADP at room temperature over the range of mean tube shear rate $41.9 \leq \bar{G} \leq 1{,}920\ s^{-1}$. This finding is consistent with previous work done in Poiseuille flow at $\bar{G} \leq 54\ s^{-1}$ with 1.0 μM ADP (Bell and Goldsmith, 1984), and in the aggregometer at 37°C with 0.5–5.0 μM ADP, collagen, or epinephrine (Coppe et al., 1981; Kelton et al., 1980). In all cases the platelets from female donors aggregated more than those from male donors. Kelton et al. (1980) attributed the sex difference to the hematocrit-dependent chelation of ionized calcium, Ca^{2+}, which occurs in citrated PRP when a 1/10 (vol/vol) dilution of the citrate anticoagulant in whole blood is routinely employed. Measurements of plasma $[Ca^{2+}]$ in this laboratory, reported elsewhere (Bell, D. N., S. Spain, and H. L. Goldsmith, submitted for publication), support this hypothesis.

We wish to acknowledge helpful discussions with Dr. T. G. M. van de Ven and Dr. M. M. Frojmovic.

This work was generously supported by grants from the Medical Research Council of Canada (MT-1835) and the Quebec Heart Foundation.

Received for publication 16 December 1988 and in final form 22 June 1989.

REFERENCES

Aasch, A. S., L. L. K. Leung, M. J. Polley, and R. L. Nachman. 1985. Platelet membrane topography: colocalization of thrombospondin and fibrinogen with the glycoprotein IIb-IIIa complex. *Blood.* 66:926–934.

Bahr, G. F., and E. Zeitler. 1965. The determination of the dry mass in populations of isolated particles. *Lab. Invest.* 14:955–977.

Bell, D. N. 1988. Physical factors governing the aggregation of human platelets in sheared suspensions. Ph.D. thesis. McGill University, Montreal, Quebec.

Bell, D. N., and H. L. Goldsmith. 1984. Platelet aggregation in Poiseuille flow. II. Effect of shear rate. *Microvasc. Res.* 27:316–330.

Bell, D. N., H. C. Teirlinck, and H. L. Goldsmith. 1984. Platelet aggregation in Poiseuille flow. I. A double infusion technique. *Microvasc. Res.* 27:297–315.

Bell, D. N., S. Spain, and H. L. Goldsmith. 1989. ADP-induced aggregation of human platelets in flow through tubes. I. Measurement of the concentration and size of single platelets and aggregates. *Biophys. J.* 56:817–828.

Belval, T., and J. D. Hellums. 1986. The analysis of shear-induced platelet aggregation with population balance mathematics. *Biophys. J.* 50:479–487.

Belval, T., J. D. Hellums, and T. Solis. 1984. The kinetics of platelet aggregation induced by shear. *Microvasc. Res.* 28:279–288.

Bennett, J. S., G. Vilaire, and D. B. Cines. 1982. Identification of the fibrinogen receptor on human platelets by photoaffinity labeling. *J. Biol. Chem.* 275:8049–8054.

Bennett, J. S., J. A. Hoxie, S. F. Leitman, G. Vilaire, and D. B. Cines. 1983. Inhibition of fibrinogen binding to stimulated human platelets by a monoclonal antibody. *Proc. Natl. Acad. Sci. USA.* 80:2417–2421.

Born, G. V. R., and M. Hume. 1967. Effects of the numbers and sizes of platelet aggregates on the optical density of plasma. *Nature (Lond.).* 215:1027–1029.

Brown, C. H., L. B. Leverett, C. W. Lewis, C. P. Alfrey, and J. D. Hellums. 1975. Morphological, biochemical, and functional changes in human blood platelets subjected to shear stress. *J. Lab. Clin. Med.* 86:462–471.

Chang, H. N., and R. Robertson. 1976. Platelet aggregation by laminar shear and Brownian motion. *Ann. Biomed. Eng.* 4:151–183.

Colantuoni, G., J. D. Hellums, J. L. Moake, and C. P. Alfrey. 1977. The response of human platelets to shear stress at short exposure times. *Trans. Am. Soc. Artif. Intern. Organs.* 23:626–631.

Coller, B. S. 1983. Biochemical and electrostatic considerations in primary platelet aggregation. *In* Surface Phenomena in Hemorheology. Their Theoretical, Experimental and Clinical Aspects. A. L. Copley and G. V. F. Seaman, editors. *Ann. NY Acad. Sci.* 416:693–708.

Coller, B. S., E. I. Peerschke, L. E. Scudder, and C. A. Sullivan. 1983. A murine monoclonal antibody that completely blocks the binding of fibrinogen to platelets produces a thrombasthenic-like state in normal platelets and binds to glycoproteins IIb and/or IIIa. *J. Clin. Invest.* 72:325–338.

Coppe, D., S. J. Wessinger, B. J. Ransil, W. Harris, and E. Salzman. 1981. Sex differences in the platelet response to aspirin. *Thromb. Res.* 23:1–21.

Corash, L., B. Shafer, and M. Perlow. 1978. Heterogeneity of human whole blood platelet subpopulations. II. Use of a subhuman primate model to analyze the relationship between density and platelet age. *Blood.* 52:727–734.

Curtis, A. S. G., and L. M. Hocking. 1970. Collision efficiency of equal spherical particles in shear flow. *Trans. Faraday Soc.* 66:1381–1390.

De Marco, L., A. Girolami, T. S. Zimmerman, and Z. Ruggeri. 1986. Van Willebrand factor interaction with the glycoprotein IIb/IIIa complex: its role in platelet function as demonstrated in patients with congenital afibrinogenemia. *J. Clin. Invest.* 77:1272–1277.

Dewitz, T. S., R. R. Martin, R. T. Solis, J. D. Hellums, and L. V. McIntire. 1978. Microaggregate formation in whole blood exposed to shear stress. *Microvasc. Res.* 16:263–271.

Frojmovic, M. M., and K. A. Longmire. 1986. Platelet aggregation in Brownian diffusion: evidence for long range interactions for human but not rabbit platelets. *Biorheology.* 23:228.

Gartner, T. K., and J. S. Bennett. 1985. The tetrapeptide analogue of the cell attachment site of fibronectin inhibits platelet aggregation and fibrinogen binding to activated platelets. *J. Biol. Chem.* 260:11891–11894.

Gear, A. R. L. 1982. Rapid reactions of platelets studied by a quenched flow approach: aggregation kinetics. *J. Lab. Clin. Med.* 100:866–886.

Goldsmith, H. L., and V. T. Turitto. 1986. Rheological aspects of thrombosis and haemostasis. Basic principles and applications. *Thromb. Haemostasis.* 55:415–435.

Haverstick, D. M., J. F. Cowan, K. M. Yamada, and S. A. Santoro. 1985. Inhibition of platelet binding to fibronectin, fibrinogen and von Willebrand factor substrates by a synthetic tetrapeptide derived from the cell binding domain of fibronectin. *Blood.* 66:946–952.

Hellums, J. D., and R. A. Hardwick. 1981. Response of platelets to shear stress—a review. *In* The Rheology of Blood, Blood Vessels and Associated Tissues. D. R. Gross and N. H. C. Hwang, editors. Sijthoff and Noordhoff, Rockville, MD. 160–183.

Holme, S., and S. Murphy. 1980. Coulter Counter and light transmission studies of platelets exposed to low temperature, ADP, EDTA, and storage at 22°. *J. Lab. Clin. Med.* 96:480–493.

Jen, C. J., and L. V. McIntire. 1984. Characteristics of shear-induced aggregation in whole blood. *J. Lab. Clin. Med.* 103:115–124.

Karpatkin, S. 1969*a*. Heterogeneity of human platelets. I. Metabolic and kinetic evidence suggestive of young and old platelets. *J. Clin. Invest.* 48:1073–1082.

Karpatkin, S. 1969*b*. Heterogeneity of human platelets. II. Functional evidence suggestive of young and old platelets. *J. Clin. Invest.* 48:1083–1087.

Kelton, J. G., P. Powers, J. Julian, V. Boland, C. J. Carter, M. Gent, and J. Hirsh. 1980. Sex-related differences in platelet aggregation: influence of hematocrit. *Blood.* 56:38–41.

Kloczewiak, M., S. Timmons, T. J. Lukas, and J. Hawiger. 1984. Platelet receptor recognition site on human fibrinogen. Synthesis and structure-function relationship of peptides corresponding to the carboxy-terminal segment of the γ chain. *Biochemistry.* 23:1767–1774.

Leung, L., and R. Nachman. 1986. Molecular mechanisms of platelet aggregation. *Annu. Rev. Med.* 37:179–186.

Marguerie, G. A., T. S. Edgington, and E. F. Plow. 1980. Interaction of fibrinogen with its receptor as a part of a multistep reaction in ADP-induced platelet aggregation. *J. Biol. Chem.* 255:154–161.

Moake, J. L., N. A. Turner, N. A. Stathopoulos, L. H. Nolasco, and J. D. Hellums. 1986. Involvement of large plasma von Willebrand factor (vWF) multimers and unusually large vWF forms derived from endothelial cells in shear stress-induced platelet aggregation. *J. Clin. Invest.* 78:1456–1461.

Moake, J. L., N. A. Turner, N. A. Stathopoulos, L. H. Nolasco, and J. D. Hellums. 1988. Shear-induced platelet aggregation can be mediated by vWF released from platelets, as well as by exogenous large or unusually large vWF multimers, requires adenosine diphosphate and is resistant to aspirin. *Blood.* 71:1366–1374.

Mundschenk, D. D., D. P. Connelly, J. G. White, and R. D. Brunning. 1976. An improved technique for the electronic measurement of platelet size and shape. *J. Lab. Clin. Med.* 88:301–315.

Newman, P. J., R. P. McEver, M. P. Doers, and T. S. Kunicki. 1987. Synergistic action of two murine monoclonal antibodies that inhibit ADP-induced platelet aggregation without blocking fibrinogen binding. *Blood.* 69:668–676.

Nichols, A. R., and H. B. Bosmann. 1979. Platelet aggregation: newly quantified using nonempirical parameters. *Thromb. Haemostasis.* 42:679–693.

Nurden, A. T. 1987. Platelet membrane glycoproteins and their clinical aspects. *In* Thrombosis and Haemostasis. M. Verstraete, J. Vermylen, R. Lijnen, and J. Arnout, editors. Leuven University Press, Leuven, Belgium. 93–125.

Paulus, J. 1975. Platelet size in man. *Blood.* 46:321–336.

Peerschke, E. I., M. B. Zucker, R. A. Grant, J. J. Egan, and M. M. Johnson. 1980. Correlation between fibrinogen binding to human platelets and platelet aggregability. *Blood.* 55:841–847.

Pennington, D. G., K. Streatfield, and A. E. Roxburgh. 1976. Megakaryocytes and the heterogeneity of circulating platelets. *Br. J. Haematol.* 34:639–653.

Plow, E. F., M. D. Pierschbacher, E. Ruoslahti, G. A. Marguerie, and M. H. Ginsberg. 1985. The effect of arg-gly-asp containing peptides on fibrinogen and von Willebrand factor binding to platelets. *Proc. Natl. Acad. Sci. USA.* 82:8057–8061.

Rand, M. L., J. P. Greenberg, M. A. Packham, and J. F. Mustard. 1981. Density subpopulations of rabbit platelets: size, protein, and sialic acid content, and specific radioactive changes following labelling with ^{35}S-sulfate *in vivo*. *Blood.* 57:741–746.

Sakariassen, K. S., P. F. E. M. Nievelstein, B. S. Coller, and J. J. Sixma. 1986. The role of platelet membrane glycoproteins Ib and IIb-IIIa in platelet adherence to human artery subendothelium. *Br. J. Haematol.* 63:681–691.

Santoro, S. A., and W. J. Lawing. 1987. Competition for related but nonidentical binding sites on the glycoprotein IIb-IIIa complex by peptides derived from platelet adhesive proteins. *Cell.* 48:867–873.

Smoluchowski, M. von. 1917. Versuch einer mathematischen Theorie der Koagulationskinetik kolloider Lösungen. *Z. Phys. Chem.* 92:129–168.

Swift, D. L., and S. K. Friedlander. 1964. The coagulation of hydrosols by Brownian motion and laminar shear flow. *J. Colloid Sci.* 19:621–647.

Timmons, S., and J. Hawiger. 1986. von Willebrand factor can substitute for plasma fibrinogen in ADP-induced platelet aggregation. *Trans. Assoc. Am. Phys.* 99:226–235.

Valdorf-Hansen, J. F., and M. B. Zucker. 1971. Effect of temperature and inhibitors on serotonin-^{14}C release from human platelets. *Am. J. Physiol.* 220:105–111.

van de Ven, T. G. M. 1982. Interactions between colloidal particles in simple shear flow. *Adv. Colloid Interface Sci.* 17:105–127.

van de Ven, T. G. M., and S. G. Mason. 1977. The microrheology of colloidal dispersions. VII. Orthokinetic doublet formation of spheres. *Colloid Polymer Sci.* 255:468–479.

von Behrens, W. E. 1972. Platelet size. Ph.D. thesis. University of Adelaide, Adelaide, South Australia.

Weiss, H. J., V. T. Turitto, and H. R. Baumgartner. 1986. Platelet adhesion and thrombus formation on subendothelium in platelets deficient in glycoproteins IIb-IIIa, Ib, and storage granules. *Blood.* 67:322–330.

Weiss, H. J., J. Hawiger, Z. M. Ruggeri, V. T. Turitto, P. Thiagarajan, and T. Hoffmann. 1989. Fibrinogen-independent platelet adhesion and thrombus formation on subendothelium mediated by glycoprotein IIb-IIIa complex at high shear rate. *J. Clin. Invest.* 83:288–297.

Yung, W., and M. M. Frojmovic. 1982. Platelet aggregation in laminar flow. Part I. Adenosine diphsophate concentration, time and shear rate dependence. *Thromb. Res.* 28:367–378.

Zeichner, G. R., and W. R. Schowalter. 1977. Use of trajectory analysis to study stability of colloidal dispersions in flow fields. *Al. Chem. Eng. J.* 23:243–254.